

# IA-FEMESH: ANATOMIC FE MODELS—A CHECK OF MESH ACCURACY AND VALIDITY

Nicole A. DeVries, Kiran H. Shivanna, Srinivas C. Tadepalli, Vincent A. Magnotta, Nicole M. Grosland

## ABSTRACT

**Musculoskeletal finite element (FE) analysis is an invaluable tool in orthopaedic research. Unfortunately, the demands that accompany anatomic mesh development often limit its utility. To ease the burden of mesh development and to address the need for subject-specific analysis, we developed IA-FEMesh, a user-friendly toolkit for generating hexahedral FE models. This study compared our multiblock meshing technique to widely accepted meshing methods. Herein, the meshes under consideration consisted of the phalanx bones of the index finger. Both accuracy and validity of the models were addressed. Generating a hexahedral mesh using IA-FEMesh was found to be comparable to automated tetrahedral mesh generation in terms of preprocessing time. A convergence study suggested that the optimal number of hexahedral elements needed to mesh the distal, middle, and proximal phalanx bones were 3402, 4950, and 4550 respectively. Moreover, experimental studies were used to validate the mesh definitions. The contact areas predicted by the models compared favorably with the experimental findings (percent error < 13.2%). With the accuracy and validity of the models confirmed, accompanied by the relative ease with which the models can be generated, we believe IA-FEMesh holds the potential to contribute to multi-subject analyses, which are pertinent for clinical studies.**

## INTRODUCTION

Computational models of joint anatomy and function provide a means for biomechanists, physicians, and physical therapists to understand the effects of repetitive motion, acute injury, and degenerative diseases. Moreover, such models may be used to improve the design of prosthetic implants. Musculoskeletal finite element (FE) analysis has proven an invaluable tool in orthopaedic-related research. While it has provided significant biomechanical insight, the demands associated with modeling the geometrically complex structures of the human body often limit its utility. The majority of the analyses reported in the literature refer to a single, or ‘average,’ bone geometry, although in many cases anthropometric variability should not be neglected. Individualized models are important for future development of this field, as they offer a means of correlating mechanical predictions with clinical outcomes. The challenge is that most biological structures are dauntingly complex and few commercial FE software programs are geared toward modeling anatomic structures. To ease anatomic mesh development, we developed IA-FEMesh,<sup>1</sup> a user-friendly toolkit for generating hexahedral FE models.

There are two broad types of mesh generation schemes—routines for structured and unstructured meshes.<sup>2,4</sup> The techniques for generating structured grids are based on rules for geometrical grid-subdivisions and mapping techniques. Structured grids, as the name implies, have a clear structure and can be recognized by all interior nodes of the mesh having an equal number of adjacent elements. The techniques used to generate them produce triangular or quadrilateral elements for two-dimensional analyses, and tetrahedral and hexahedral elements in three-dimensions. Structured meshing algorithms generally involve complex iterative smoothing techniques that attempt to align elements with boundaries or physical domains. Where non-trivial boundaries are required, “block-structured” techniques can be employed which allow the user to break the domain up into topological blocks. Structured grid generators are most commonly used when strict elemental alignment is mandated by the analysis code or is necessary to capture physical phenomenon. Unstructured mesh generation, on the other hand, relaxes the node valence requirement, allowing any number of elements to meet at a single node. Triangle and tetrahedral meshes

---

The University of Iowa, Iowa City, IA 52242

### Corresponding Author:

Nicole M. Grosland, Ph.D.  
Department of Biomedical Engineering  
Department of Orthopaedics and Rehabilitation  
Center for Computer Aided Design  
1418 Seamans Center  
The University of Iowa  
Iowa City, IA 52242  
319-335-6425 (Tel.)  
319-335-5631 (Fax)  
nicole-grosland@uiowa.edu

are most commonly thought of when referring to unstructured meshing. While there exists some overlap between structured and unstructured mesh generation technologies, the main feature that distinguishes the two approaches is the unique iterative smoothing algorithm(s) employed by structured grid generators. While free-form meshing schemes using tetrahedral elements are widely employed, it is well known that hexahedral elements would, in many cases, be more effective for analysis.

IA-FEMesh<sup>1</sup> is based on a multiblock approach. The objective of this study was to address the accuracy, validity, and quality of the models generated via the building block approach provided by IA-FEMesh. Moreover, we compared the resulting mesh definitions to both hexahedral and tetrahedral meshes generated via commercial software packages. For this study, the phalanx bones of the index finger were used to develop and test the methodology; the phalanx bones are small and have regions of high curvature, which tested the capabilities of IA-FEMesh to capture these anatomical features.

## METHODS

### Specimen

A cadaveric arm (female, age = 74) was obtained from the Anatomy Gifts Registry in Hanover, Maryland. Computed tomography (CT) images were obtained on a Siemens Sensation 64 CT scanner (matrix = 512x512, FOV = 172mm, KVP = 120, Current = 94mA, Exposure = 105mAs) with an in-plane resolution of 0.34mm and a slice thickness of 0.4mm. Following image acquisition, the data was processed using BRAINS2 software<sup>5,6</sup>. The images were resampled to 0.2mm isotropic voxels and spatially normalized such that the vertical plane of the frame was aligned superiorly/inferiorly in the coronal view, vertically aligning the third metacarpal. The CT images were manually segmented<sup>7</sup> to isolate the phalanx bones of the index finger and the respective bony surface representations were exported in STL format as triangulated surfaces (Figure 1a). These surfaces formed the foundation for the respective mesh definitions.

### Mesh Generation using IA-FEMesh

The first step toward meshing the bones was to define building block structures for each of the bony surface definitions. For example, the initial building block for the distal bone was defined by the bounds of the surface (Figure 1b). This block was then edited to better mimic the surface geometry. This was done by subdividing the block and repositioning the block vertices closer to the surface geometry (Figure 1c). Once the structure was defined, mesh seeding was assigned to the blocks

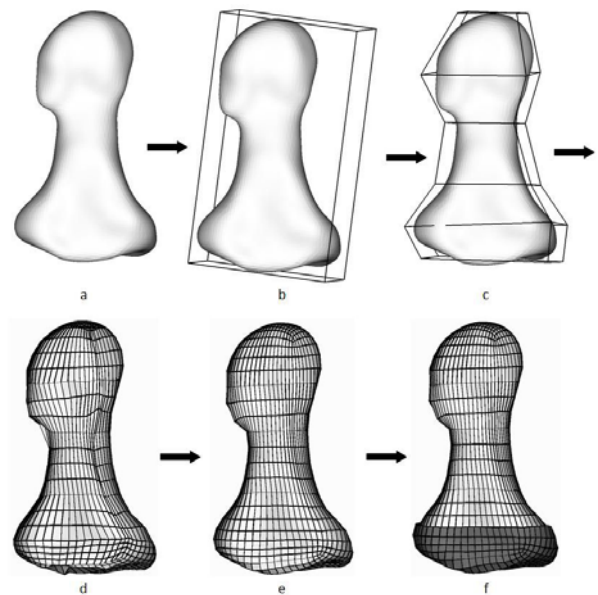


Figure 1. An example of the meshing techniques used on the distal phalanx bone. IA-FEMesh initiates with (a) a surface representation and (b) an initial building block is defined based on the bounds of the surface. This block is then (c) subdivided into multiple building blocks and edited to match the surface geometry. Mesh seeding is applied and projected onto the surface to create (d) an initial, unsmoothed hexahedral mesh. This mesh is (e) smoothed using Laplacian smoothing. Then (f) a uniform articular cartilage layer is extruded.

based on an average element length. The mesh was then projected onto the surface (Figure 1d) and smoothed to accommodate distorted elements caused by areas of high curvature (Figure 1e). A detailed description of IA-FEMesh is described by Grosland and colleagues.<sup>1</sup>

### Model Accuracy

Prior to implementing any FE model, it is important to ensure that the FE mesh used to partition the domain of interest is of sufficient spatial resolution to provide the desired degree of accuracy. This process consists of progressively increasing the mesh resolution to the point where the mesh is adequately refined such that the solution does not change appreciably with additional mesh refinement. In other words, the mathematical solution has converged. Consequently, a convergence study was performed for each of the phalanx bones of the index finger under consideration.

A hexahedral mesh of each phalanx bone was generated in IA-FEMesh as described previously. Various levels of mesh refinement were considered; this was accomplished by varying the average element length between 0.25mm and 2.0mm. For simplicity, the bone was considered an elastic, isotropic material with an

elastic modulus of 2.0GPa and Poisson's ratio of 0.35. A 40N (grasp strength<sup>8</sup>) point load was applied at the phalanx head, while the proximal end of the bone was fixed in all directions. All analyses were performed using ABAQUS/Standard (Version 6.7-1; Hibbit, Karlsson & Sorensen, Inc, Pawtucket, RI). The ideal mesh was determined when the von Mises stresses converged; the stresses were monitored at the distal end, mid shaft, and proximal end of each bone at regions away from the boundary and loading conditions where high stress concentrations occur.

### Comparing Meshing Techniques

Mesh development via IA-FEMesh was compared to conventional meshing techniques afforded by commercial (MSC/PATRAN, Version 2005 r2; MSC Software Corporation, California, USA) and open-source (NETGEN, Version 4.3) software. This allowed for a direct comparison of the multiblock meshing technique to methods that are widely accepted and utilized. Several factors were considered including the time to generate the mesh. This time did not include the time to segment the CT image or generate the surface definition, since each mesh initiated with the same surface.

Additionally, element types (hexahedral and tetrahedral) were compared with respect to the required mesh density and the mesh quality. Note, NETGEN does not allow the user to assign a given mesh density, but instead defines refinement on a scale of "very coarse" to "very refined." In terms of mesh quality, the number of zero volume and distorted elements, as defined by ABAQUS, were investigated. In addition, the ability to capture the anatomical geometry, specifically at the articulations and areas of high curvature, and the resultant von Mises stress distributions were studied.

### Contact Analysis

The distal interphalangeal (DIP) joint, due to its small size, was the focus of our contact analysis/validation studies. Subject-specific material properties were assigned to the middle and distal phalanx bone meshes using the established relationship between apparent density and the modulus of elasticity.<sup>9</sup> A Poisson's ratio of 0.35 was assigned to all bony elements.

In addition to the bones, the articular cartilage was modeled for contact analysis. Due to the size of the joint space, the cartilage could not be readily defined from imaging data. Therefore, the cartilage was created based on the underlying bone mesh, by extruding the cartilage elements a given distance. This resulted in a uniform cartilage layer (two layers of elements) 0.25mm thick. Figure 1f shows an example of the distal phalanx bone

and the corresponding articular cartilage hexahedral mesh for the DIP joint. The cartilage was considered as an elastic, isotropic material with a modulus of elasticity of 12.0MPa and a Poisson's ratio of 0.42.

The middle bone was fixed in all directions (x,y,z) at the proximal-most nodes; the distal bone was loaded with respect to the anatomical center of rotation of the DIP joint. Initially, a 10N compressive follower load was applied while the distal bone was free to translate and rotate. This translational and rotational freedom allowed the bone to settle in the most natural position. Once the bone settled, the distal bone was fixed in the x and z translations, as well as all rotations. A compressive force was applied until the maximum loading was obtained. The maximum load was defined by the load at which the solution failed to converge based on the given boundary conditions.

### Model Validity

To validate the FE contact models, biomechanical testing of the corresponding specimen was conducted. The bones of the index finger were dissected of all soft tissues with the exception of the ligaments and articular cartilage. The ligaments were originally kept intact to aid joint stability. Once joint malalignment had been accounted for, the ligaments were removed to accommodate pressure sensitive film within the joint space.

A custom fixation device was used to anchor the bones for quasi-static loading using an MTS 858 Mini Bionix II system and gimbal that allowed for axial loading, abduction/adduction, and flexion/extension. A custom lockable XZ table was employed to adjust for slight malalignments prior to applying large loads. Note that the loading and boundary conditions described above for the FE analysis mimicked those applied experimentally.

The distal bone was fixed in the gimbal and the middle bone was fixed and attached to the XZ table. A pre-load was initially applied, allowing the joint to settle in the neutral position and account for any malalignments. Once settled, the XZ table was locked, allowing no translation upon further loading. The specimen load was released to insert pressure film in order to capture the contact area. This study used both super low pressure film (0.5-2.5MPa) and low pressure film (2.5-10MPa). Axial compressive loads of 25N and 50N were applied. This process was repeated three times for each load. The pressure film was scanned using an HP Scanjet 4070 Photosmart scanner and the contact area was measured using ImageJ (Version 1.40g; Research Services Branch, National Institute of Mental Health, Bethesda, MD).

**TABLE 1**

Based on the convergence study, the ideal number of elements and nodes for each phalanx bone, as well as the average element length used to obtain the ideal meshes

Finger Bone	Number of Nodes	Number of Elements	Average Element Length (mm)
Distal Phalanx	4200	3402	0.625
Middle Phalanx	5952	4950	0.75
Proximal Phalanx	5544	4550	1.0

**RESULTS**

Table 1 summarizes the number of nodes, number of elements, and average element length that was deemed optimal for each bone based on the convergence study.

**Meshing Technique and Element Comparison**

Using IA-FEMesh it took approximately six minutes to generate a hexahedral mesh of the proximal phalanx bone. This was comparable to NETGEN, which allowed the same bone to be meshed in four minutes via tetrahedral elements. PATRAN, however, required significantly more time. Table 2 summarizes the mesh generation time for each meshing technique and element type, in addition to the resulting element quality.

The mesh generated using IA-FEMesh resulted in fewer distorted hexahedral elements (i.e., 10%), as compared to the model created in PATRAN (16.58%, including one zero volume element). Both hexahedral meshes had more distorted elements (angles less than 45° or greater than 135°) than the tetrahedral mesh, mainly along the edges of the bone.

Overall, the meshes had similar stress distributions, as shown in Figure 2. The tetrahedral meshes required considerably more elements to obtain smoother stress distributions in comparison to the hexahedral meshes.

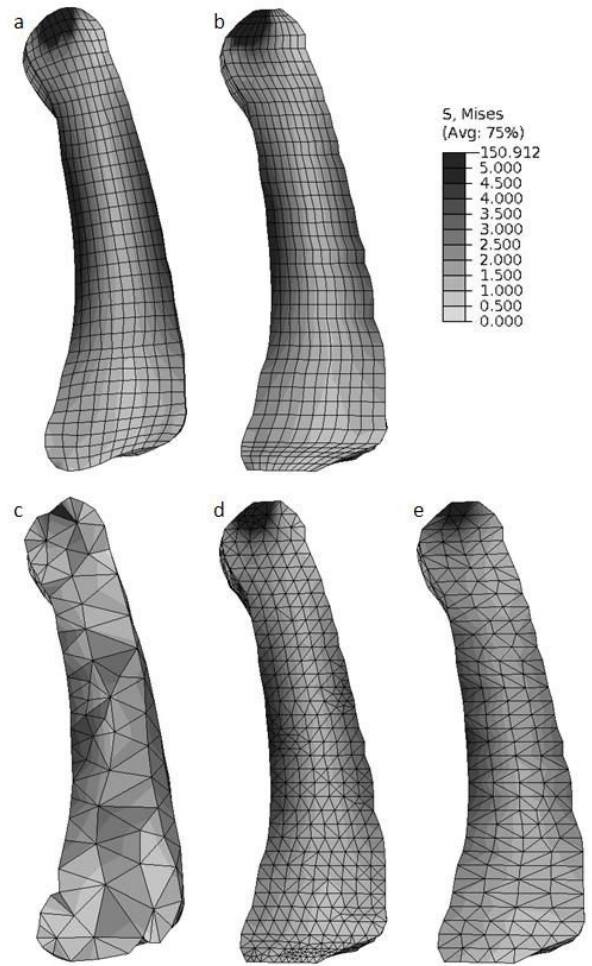


Figure 2. The von Mises stress distribution for the various meshing techniques: (a) IA-FEMesh and (b) PATRAN hexahedral mesh, (c) NETGEN tetrahedral mesh (moderate), and PATRAN (d) tetrahedral mesh, and (e) tetrahedral mesh (2.0 mm). Meshes have an average element length of 1.0 mm unless stated otherwise.

**TABLE 2**

The number of nodes and elements in each mesh and the corresponding average element length as well as element quality and mesh generation time

Meshing Software	Element Type	Average Element Length (mm)	Number of Nodes	Number of Elements	Distorted Elements	Zero Volume Elements	Mesh Generation Time (min)
IA-FESMesh	Hex	1	5544	4550	455	0	6
PATRAN	Hex	1	6552	5434	901	1	330
PATRAN	Tet	1	11366	52835	228	0	330
PATRAN	Tet	2	1724	7506	55	0	330
NETGEN	Tet	—	808	2457	0	0	1

Note: Hex = C3D8, Tet - C3D4 element types in ABAQUS

**TABLE 3**  
**The resulting contact area for the experimental data and the finite element model**

Load (N)	Contact Area (mm <sup>2</sup> )		
	Pressure Film	FE Model	Error (%)
25	12.36	10.73	-13.17
50	15.61	15.03	-3.69

This is most noticeable in the mesh generated using NETGEN; the stress distribution is not as smooth for this coarse mesh. Additionally, IA-FEMesh and NETGEN provided the most geometrically accurate meshes with the ability to capture the articulating surface and areas of curvature; whereas the geometry defined using PATRAN did not capture the articulating surface, but instead a flat surface was generated. For contact analysis, the geometry of the articulating surface is crucial.

**Contact Analysis**

Table 3 summarizes the experimental and computational contact areas (and the corresponding percent error) for the DIP joint at the 25N and 50N compressive loads. Figure 3 illustrates the contact area predicted via the FE analysis. As compared to the experimental findings, the FE model underestimated the contact area for both loading conditions. As the load increased from 25N to 50N, the percent error decreased from 13.17% to 3.69%. These values are similar to the error values reported by Harris et al.<sup>10</sup> and Liau et al.<sup>11</sup> They have shown that Fuji film percent error ranges from 8-36% for contact area measurements.

**DISCUSSION**

**Mesh Comparison**

The time to generate an accurate finite element model is crucial when considering subject-specific models. IA-FEMesh enabled geometrically accurate hexahedral meshes to be readily developed (approximately six minutes). This was considerably less time intensive than traditional methods such as PATRAN, which proved time consuming and laborious. Meshing algorithms such as NETGEN are capable of rapidly generating a mesh, but are limited to tetrahedral elements. Moreover, NETGEN has limited control over the level of mesh refinement. The meshing technique utilized by NETGEN requires the meshes to be optimized and due to the curvature of the bony surface and the increased number of elements, NETGEN could not optimize a more refined mesh. The bony geometry proved challenging for PATRAN as well. PATRAN relies on a series of segmented contours, as

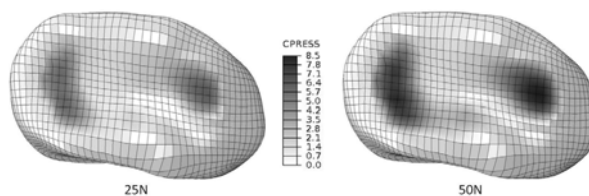


Figure 3. The finite element predicted contact pressure for the distal interphalangeal joint at 25N and 50N loads.

opposed to the surface representation, as its structural input. Consequently, the plane in which the contours were defined played a significant role in the outcome of the mesh. Herein, the contours were defined axially, and as a result yielded poor surface definitions under these conditions. Had the models generated by PATRAN been considered for contact analysis, the contours would have been exported in another plane (e.g., coronal). That being said, the palmar and/or dorsal side of the mesh would have then lacked fidelity. Consequently, both IA-FEMesh and NETGEN benefit from relying on the bony surface representation to generate the mesh.

It should be noted that as the geometric complexity increases, the time required to generate the building block structure in IA-FEMesh will increase, thereby adding time to the meshing process. Tetrahedral algorithms, however, would not be influenced significantly. That being said, the time to mesh the same model via traditional hexahedral methods would also likely increase substantially, thus making IA-FEMesh a favorable alternative for hexahedral mesh definitions. To date, no attempt has been made to optimize the number of building blocks necessary for meshing a given structure. Future studies will investigate, for example, the fewest number of blocks required to mesh a bone. Moreover, our long-term goal is to automate the building block definitions, thereby further reducing the time devoted to establishing the building block structures.

The mesh generated using IA-FEMesh resulted in fewer distorted hexahedral elements as compared to the model created in PATRAN, however both hexahedral meshes had more distorted elements than the tetrahedral meshes. This was expected, since tetrahedral elements are less sensitive to distortion.<sup>12</sup>

When comparing the stress distributions for the various models, the hexahedral meshes yield a smooth stress distribution as compared to the tetrahedral mesh definitions. A tet mesh oftentimes results in an irregular pattern of elements, with considerable variation in element shape. And, as is true with elements in general, as the element shape deviates from ideal, numerical integration problems arise and inaccuracies are introduced. It takes approximately five times more tetrahedral elements (~27,000) than hexahedral elements (~5,000)

to obtain a similar distribution. Due to the mesh refinement limitations imposed by NETGEN, a suitable mesh contour was not achieved.

### Contact Analysis

This work was an extension of a previous study conducted by Gassman.<sup>13</sup> Therein, the phalanx bones were treated as rigid bodies and the articular cartilage was modeled with eight-noded continuum elements with an elastic modulus of 12.5MPa and Poisson's ratio of 0.42. Axial loading was applied using point loading, ranging from 5N to 25N. The loading conditions resulted in contact areas ranging from approximately 5mm<sup>2</sup> to 25mm<sup>2</sup> for the DIP articulation. This study utilized continuum elements throughout with subject-specific material properties and showed similar results, predicting contact area ranging from 10.7 to 15.0mm<sup>2</sup> for the DIP joint with compressive loads of 25N and 50N, respectively.

The percent error for the DIP joint loaded under compression to 25N and 50N was 13.17% and 3.69%, respectively. Harris et al.<sup>10</sup> and Liau et al.<sup>11</sup> have shown that the percent error for Fuji film when measuring contact area can range from 8-36%. Our results fall within and below this reported error range. We believe that our results could be further improved upon with slight modifications. For example, the choice of pressure sensitive film (super low pressure and low pressure films) may have influenced the outcome. For example, ultra low films may have been preferable to capture contact pressures as low as 0.2 MPa.

As with any mathematical or computational model, assumptions were made. For example, in the absence of imaging data detailing the cartilage, this model assumed a uniform cartilage thickness over the articular surface; when in actuality there is variation over the articulation. Consequently, this may too influence the resulting contact of the joint. Despite these assumptions, the results were in agreement with the experimental findings, thereby establishing confidence in the validity of the mesh.

### CONCLUSION

Finite element modeling is an invaluable tool for biomechanical research. Until recently, the process of generating accurate hexahedral meshes for contact analysis was time consuming and labor intensive. This study found that IA-FEMesh is capable of generating anatomically accurate hexahedral meshes of the human phalanx in significantly less time than a traditionally used commercial mesh generator; in addition, the time is comparable to tetrahedral meshing techniques such as NETGEN. Since IA-FEMesh allowed for easy mesh generation, it was utilized to create meshes for contact analy-

sis of the distal interphalangeal joint. Moreover, these models were validated experimentally using pressure sensitive film. Therefore, IA-FEMesh has been shown to be a user-friendly meshing software that efficiently generates accurate finite element models comparable to the labor intensive traditional meshing techniques.

### ACKNOWLEDGMENTS

This project was funded by awards R21EB001501 and R01EB005973 from the National Institute of Biomedical Imaging and Bioengineering, National Institute of Health, as well as a National Science Foundation Graduate Fellowship.

### REFERENCES

1. **Grosland N, Shivanna K, Magnotta V, et al.** IA-FEMesh: An open-source, interactive, multiblock approach to anatomic finite element model development. *Computer Methods and Programs in Biomedicine* In press 2008.
2. **Bornemann F, Erdmann B, Kornhuber R.** Adaptive Multilevel Methods in Three Space Dimensions. *International Journal of Numerical Methods in Engineering* 1993;36:3187-3203.
3. **George P.** *Automatic Mesh Generation*. ed: John Wiley & Sons, 1993.
4. **Mitchell S, Vavasis S.** Quality Mesh Generation in Three Dimensions. 8th ACM Conference on Computational Geometry, 1992.
5. **Andreasen NC, Cohen G, Harris G, et al.** Image processing for the study of brain structure and function: problems and programs. *Journal of Neuropsychiatry & Clinical Neurosciences* 1992;4:125-133.
6. **Magnotta VA, Harris G, Andreasen NC, et al.** Structural MR image processing using the BRAINS2 toolbox. *Computerized Medical Imaging and Graphics* 2002;26:251-264.
7. **DeVries N, Gassman E, Kallemeyn N, et al.** Validation of phalanx bone three-dimensional surface segmentation from computed tomography images using laser scanning. *Skeletal Radiology* 2008;37:35-42.
8. **Moran J, Hemann J, Greenwald A.** Finger Joint Contact Areas and Pressures. *Journal of Orthopaedic Research* 1985;3:49-55.
9. **Carter D, Hayes W.** The compressive behavior of bone as a two-phase porous structure. *Journal of Bone and Joint Surgery* 1977;59:954-962.
10. **Harris ML, Morberg P, Bruce WJ, et al.** An improved method for measuring tibiofemoral contact areas in total knee arthroplasty: a comparison of K-scan sensor and Fuji film. *Journal of Biomechanics* 1999;32:951-958.

11. **Liau JJ, Cheng CK, Huang CH, et al.** Effect of Fuji pressure sensitive film on actual contact characteristics of artificial tibiofemoral joint. *Clinical Biomechanics* 2002;17:698-704.
12. Solid (Continuum) Elements. Analysis User's Manual: Elements. 6.5 ed: ABAQUS, Inc, 2004:14.11.11-11 - 14.11.11-20.
13. **Gassman EE.** The Validation of an Automated Image Segmentation Technique for the Development of Anatomic Finite Element Models. Biomedical Engineering. Iowa City: The University of Iowa, 2006:112.